

# Improvement of the contact resistance by annealing in organic photovoltaic devices

GUILIN LIU<sup>c</sup>, YING GUO<sup>a</sup>, HUIMIN YAN<sup>a</sup>, JIAQI WU<sup>b</sup>, WENJIA LI<sup>a</sup>, XI XI<sup>b</sup>, YIXIN ZHANG<sup>a</sup>, GUOHUA LI<sup>a,d,\*</sup>

<sup>a</sup>*School of Science, Jiangnan University, Wuxi 214122, China*

<sup>b</sup>*Suntech Power Co., Ltd. Wuxi 214028, China*

<sup>c</sup>*School of Internet of Things Engineering, Jiangnan University, Wuxi 214122, China*

<sup>d</sup>*Jiangsu (Suntech) Institute for Photovoltaic Technology, Wuxi 214028, China*

The annealing process was used to decrease the contact resistance of organic solar cells, in which Zinc Phthalocyanine (ZnPc) was used as the active layer. The contact resistance was significantly improved by using the proper annealing temperature and duration in this experiment. The change of morphology between organic layer and anode was observed after the annealing process. In this study, the contact resistance decreased by 8% for a treatment at 120°C for 20 minutes compared with that of new prepared samples.

(Received May 15, 2012; accepted October 30, 2012)

**Keywords:** Organic solar cells, Annealing process, Contact resistance, Morphology

## 1. Introduction

Since 1970s, organic photovoltaic devices have been attracting a great deal of attention because of their flexibility, low cost, light weight and potential applications [1, 2]. After Tang [3] made the first double-layer structured solar cell in 1986, there has been a growing interest in studying the properties of organic semiconductors and their potential applications. In fact, organic devices have large resistance [4] including bulk resistance [4-6] and contact resistance [7-9]. The bulk resistance [10] will remain constant unless a chemical reaction occurs. Meanwhile, organic materials with  $\pi$ -conjugated system are connected by weak interaction among molecules. The phenomenon results in the hopping conduction mechanism [11], which is an important reason for high bulk resistance of organic materials. Due to different energy levels [12, 13] of materials, the contact resistance cannot be neglected on the power conversion efficiency (PCE) of organic solar cells. Hence, many groups paid their attention on modifying cathode [14], such as having a buffer layer inserted between cathode and organic materials or using some kind of new organic materials [8, 10, 15, 16]. But until now there is rarely attention has been paid on anode modification [17-19].

Annealing process has been already widely used in the preparation of inorganic solar cells. It benefits to the improvement of interface [20] and traps [21]. By using annealing method, Saleh et al. [22] gives a hole concentration of about  $5.5 \times 10^{17} \text{ m}^{-3}$ , this value drops down by more than one order of magnitude to  $2.7 \times 10^{16}$

$\text{m}^{-3}$  for thermally treated sample. This is only 20 times less than the free hole concentration in an un-treated film due to the desorption of oxygen molecules from the surface of the zinc phthalocyanine (ZnPc) films, which acts as acceptor-like centers [23, 24]. However, there is still no study of annealing method on surface morphology and contact resistance. In this work, an annealing process is utilized to enhance the performance of photovoltaics, and the results show the contact resistance decreases under appropriate time and temperature.

## 2. Experiment

### 2.1 Fabrication of samples

The samples were fabricated in a typical sandwich structure, as shown in Fig. 1. The ITO-glass substrates (with a sheet resistance of  $7 \Omega/\text{cm}^2$ ) were sequentially cleaned by ultrasonic treatment in acetone, isopropyl alcohol, and di-ionized water, then treated by UV-ozone for 15 min after being blown by  $\text{N}_2$  gas. The UV wavelength used here was 185 nm with the power of 20W. The temperature and humidity inside the box were kept at 20 °C and 30%, respectively. The purity of ZnPc used was 98.5%+ (AG) supplied by Fluka, which was not further purified before experiments. All layers were fabricated by vacuum evaporation at a pressure of  $6 \times 10^{-3}$  Pa. Thicknesses were 60 and 200 nm for ZnPc and Al respectively, monitored by a quartz oscillator thickness

monitor. They were also checked by an ellipsometer (produced by Gaertner Scientific Corporation).

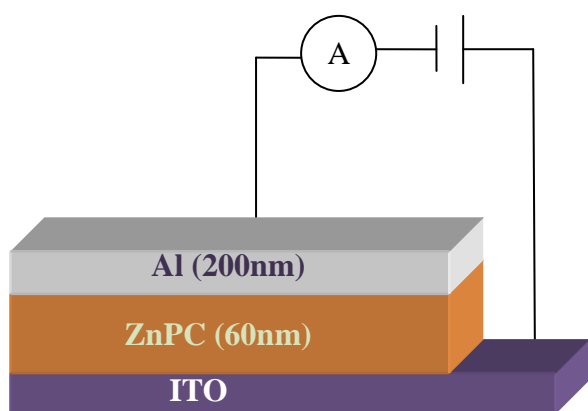


Fig. 1. Schematic structure of samples.

## 2.2 Characterization measurement

The annealing process was undertaken in Glove box (Mikrouna universal 1800) in Nitrogen atmosphere after the evaporation of aluminum. In order to ensure the accuracy and the repeatability of the experiment [25-29], four tests were divided into A & B series. Table 1 shows the details of A & B series. The measurements were taken under an illumination of 100 mW/cm<sup>2</sup> (monitored by a standard polysilicon solar cell) with an AM 1.5G solar simulator (San-EI XES-151S). The current-voltage characteristics (*I-V*) for those samples were investigated by using four wires measuring method (Keithley 2400 sourcemeter) in order to eliminate the effects of the contact barrier. The conductivity tests were carried out by applying -0.5 V to 0.5 V on the electrodes. All the characteristic parameters in Table 1 are averaged with 8 samples. The interface morphology between ITO and ZnPc was observed by Laser Scanning Microscope (Keyence VK-9710).

Table 1. Parameters of samples.

Samples	<i>d</i> (nm)	<i>l</i> (mm)	<i>w</i> (mm)	<i>T</i> (°C)	<i>t</i> (min)
A <sub>0</sub>	60 ± 3	5 ± 0.1	4 ± 0.1	120	0
A <sub>1</sub>	60 ± 3	5 ± 0.1	4 ± 0.1	120	10
A <sub>2</sub>	60 ± 3	5 ± 0.1	4 ± 0.1	120	20
A <sub>3</sub>	60 ± 3	5 ± 0.1	4 ± 0.1	120	30
A <sub>4</sub>	60 ± 3	5 ± 0.1	4 ± 0.1	120	40
B <sub>1</sub>	60 ± 3	5 ± 0.1	4 ± 0.1	100	20
B <sub>2</sub>	60 ± 3	5 ± 0.1	4 ± 0.1	120	20
B <sub>3</sub>	60 ± 3	5 ± 0.1	4 ± 0.1	150	20
B <sub>4</sub>	60 ± 3	5 ± 0.1	4 ± 0.1	180	20

*d*, film thickness; *l*, film length; *w*, film wide; *T*, temperature of annealing process; *t*, annealing time.

## 3. Results and discussion

Matthew [6-8, 11] studied the resistivity of organic devices, and explained it by equation 1. The resistivity was measured in Ω/mm

$$\rho = \frac{1}{ne\mu_p} \quad (1)$$

Where,  $\rho$  is the resistivity of the organic layer; *n* is the number of holes. As ZnPc is a p type material,  $\mu_p$  is the mobility of holes. Then, the bulk resistance was calculated by equation 2

$$R_B = \rho \frac{l}{(w \times d)} \quad (2)$$

$R_B$  is the value of bulk resistance; *l* is the length of the organic layer; *w* and *d* are the width and thickness of samples, respectively.

### 3.1 A series

In A series, samples were annealed for 0, 10, 20, 30 and 40 minutes respectively to find the best annealing time. During the measurement the humidity (15%) and temperature (25°C) conditions were kept as constant. An Ohmic current ( $J \propto V$ ) was observed at low applied voltages.

The resistance values are shown in Table 2. After 10 minutes treatment, the contact resistance significantly decreases. Then the contact resistance achieves to the minimum value when the time of annealing process extends to 20 minutes. However, the result of annealing time of 30 minutes is obviously worse than that of 20 minutes because the interface is destroyed by long time heating. Therefore, these experimental results indicate a best time for annealing process is 20 minutes.

Table 2. Resistance of A series. Total resistance ( $R_T$ ); bulk resistance ( $R_B$ ); contact resistance ( $R_C$ ); annealing time ( $T$ ).

Numbers	$R_T(\Omega)$	$R_B(\Omega)$	$R_C(\Omega)$	$T(\text{min})$
A <sub>0</sub>	584.79	115.83	468.96	30
A <sub>1</sub>	202.34	115.91	86.43	30
A <sub>2</sub>	153.30	115.84	37.46	30
A <sub>3</sub>	244.25	115.76	128.49	30
A <sub>4</sub>	584.75	115.64	468.11	30

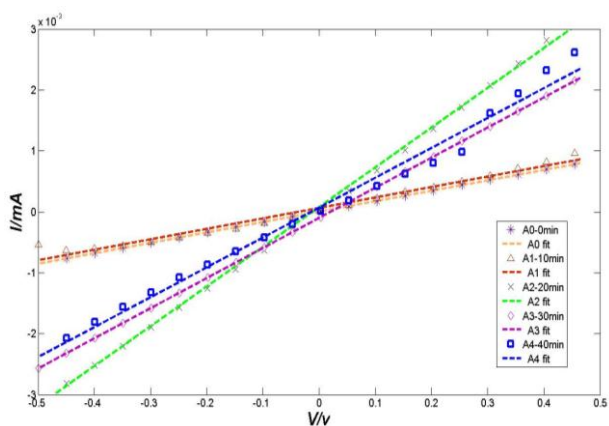


Fig. 2. I-V curve of different annealing time/the annealing temperature was kept at 120 °C experimental data were fitted using matlab software. The samples were exposed in the air without illumination, while the temperature was kept at 25 °C and the humidity was kept below 15%. All the photovoltaic characteristics were measured under an illumination of 100 mW/cm<sup>2</sup> with an AM1.5G solar simulator.

Fig. 2 shows I-V curve for samples annealed for different times. The results here are the same as those in Table 2. 20 minutes treatment is also proved to be the best annealing time for organic photovoltaic devices in this experiment. As annealing process recrystallize the active layer, molecules will change locations and phase to decrease desorption [20, 21, 28]. This phenomenon directly results in low density of trapping centers and

electrodes can collect more carriers after annealing process. There still has a large resistance for A<sub>0</sub> and A<sub>1</sub>. But longer annealing time will destroy the arrangement of molecules with a worse surface morphology, which will make carriers difficult to get through the interface. Hence, A<sub>3</sub> and A<sub>4</sub> also have large resistance [10].

### 3.2 B series

The annealing time was set for 10 minutes by varying temperature of 100 °C, 120 °C, 150 °C and 180 °C to find out the optimal annealing temperature.

The results are listed in Table 3. After being annealed at 100 °C, the contact resistance significantly decreases. As the temperature of annealing process increases to 120 °C, the samples achieve the best performance because of a rougher interface. However, the result of applying 150 °C condition is slightly worse than that of 120 °C. Therefore, these experimental results show the best temperature for annealing process is 120 °C.

Table 3. Resistance of B series. Total resistance ( $R_T$ ); bulk resistance ( $R_B$ ); contact resistance ( $R_C$ ).

Numbers	$R_T(\Omega)$	$R_B(\Omega)$	$R_C(\Omega)$
B <sub>1</sub>	260.69	115.88	144.81
B <sub>2</sub>	202.34	115.93	86.41
B <sub>3</sub>	211.86	115.72	96.14
B <sub>4</sub>	551.88	115.75	436.13

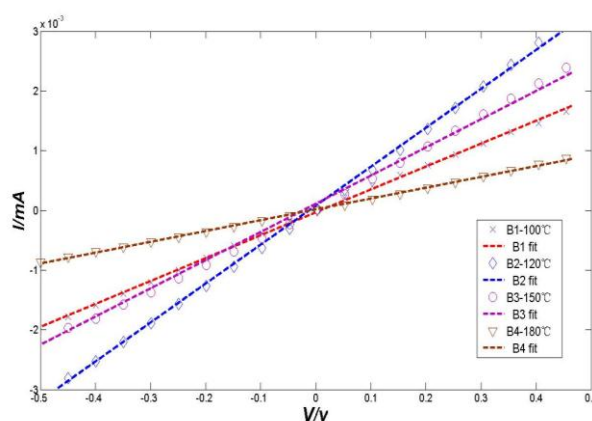


Fig. 3. I-V curve of different annealing temperatures/the annealing time was kept for 10 min, experimental data were fitted using matlab software. The samples were exposed in the air without illumination, while the temperature was kept at 25 °C and the humidity was kept below 15%. All the photovoltaic characteristics were measured under an illumination of 100 mW/cm<sup>2</sup> with an AM1.5G solar simulator.

Similarly, Fig. 3 shows that the contact resistance needs an appropriate temperature to change location and phase of the molecules. The curve shows the same conclusion as Table 3 indicates. B<sub>2</sub> shows the lowest resistance. As being mentioned previously, these results also exhibit that annealing process has changed the interface between ITO and organic layer.

### 3.3 Improvement of surface morphology

To get deeper insight into these phenomena of resistance variation, laser scanning microscope (LSM) images were compared with each other. Photoelectric response and dipole excitons are generated in organic layer while conjugated molecules absorb photons. Photovoltaic effect is formed after excitons separated into effective carriers, otherwise, they will be recombined by impurities absorption and molecular oscillation [24, 29-34]. As excitons being separated, the carriers need to be collected by electrodes, while they are crossing traps by hopping conduction.

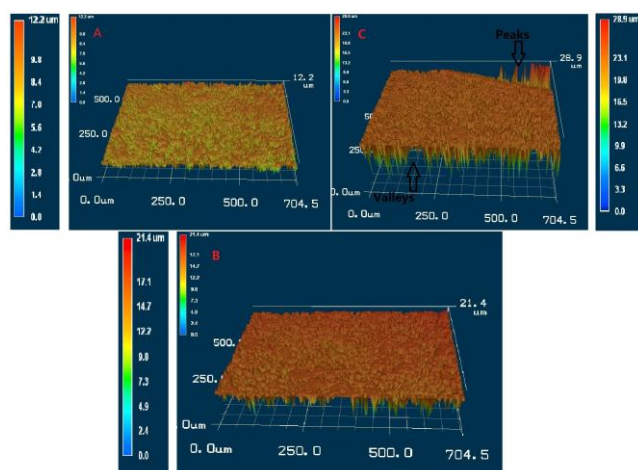


Fig. 4. Surface morphology of samples. A : ( un-annealed sample); B :(best annealed sample); C : (sample with high temperature & long time annealing process).

Fig. 4 shows the surface morphology between ITO and ZnPc with different annealing process. The interface is quite different owing to different energy injection. Obviously, the un-annealing samples (sample A<sub>0</sub>) is neatly stacked as shown in Fig. 4 A, as the Root Mean Square (RMS) value shows, the interface between substances is not integrated closely. Fig. 4 B shows a rougher surface (sample A<sub>2</sub>) at 120°C. The interface is better than that of the un-annealed one. The organic molecules sufficiently fill on ITO surface because the energy injection makes the molecular interaction and chemical bonds be rearranged [29, 30]. This makes holes get to anode before being

trapped by traps, which coincides with the decreasing of contact resistance. When annealing process continues (sample A<sub>4</sub>), the surface will be seriously damaged as shown in Fig. 4 C. It means annealing process needs an appropriate annealing temperature and time. Long time and high temperature will result in destruction of the surface morphology. As energy injection, more and more molecules will be deviated from the bondage of molecular inter-atomic forces and bonding forces. Those molecules will rearrange and secondary reunion phenomenon will happen. Because of dislocations, carriers cannot pass the contact interface which leads to a large resistance. Thus, there is a best annealing process as Fig. 4 B shows. These samples have an appropriate interface for holes to transport before recombination.

### 4. Conclusion

In summary, in this paper, the contact resistance with the existence of annealing process was investigated. An Ohmic conduction was observed during measurements. The reason for the variation of conductivity is the improvement of the surface morphology. It is found that the minimum resistance is obtained when samples are annealed at 120 °C for 20 minutes due to the best surface morphology. An appropriate annealing process will make those substances integration closely and that will benefit to carrier transportation, which leads to the decrease of contact resistance. These results indicate that the treatment for organic layer is an attractive approach for improving the power conversion efficiency.

### References

- [1] C. Lungenschmied, G. Dennler, H. Neugebauer, S. N. Sariciftci, M. Glatthaar, T. Meyer, A. Meyer, *Solar Energy Material and Solar Cells*, **91**, 379 (2007).
- [2] F. C. Krebs, *Solar Energy Material and Solar Cells*, **93**, 465 (2009).
- [3] C. W. Tang, *Applied Physics Letters*, **48**, 183 (1986).
- [4] M. Klessinger, J. Michl, New York: VCH Publishers, Inc. 1995.
- [5] G. Yongli, *Materials Science and Engineering*, **68**, 39 (2010).
- [6] O. R. Matthew, A. G. Suren, J. Mikkil, *Solar Energy Materials and Solar Cells*, **95**, 1253 (2011).
- [7] A. Stéphane, C. Raphaël, G. Romain, *Organic Electronics*, **12**, 897 (2011).
- [8] V. Vincenzo, L. R. Manuela, N. Donatai, *Organic Electronics* **10**, 1074 (2009).
- [9] Y. Hajime, K. Daigo, S. Naoki, M. Shin-ichi, *Solar Energy Materials and Solar Cells*, **6-7**, 976 (2009).
- [10] S. Yang, L. Kejia, M. Nabanita, *Solar Energy Materials and Solar Cells*, **95**, 2314 (2011).
- [11] A. Z. Natalya, R. P. Mark, *Physics Reports*, **509**, 1

- (2011).
- [12] S. Yukutake, T. Kawazoe, T. Yatsui, W. Nomura, K. Kitamura, M. Ohtsu, *Applied Physics B* **3**, 415 (2010).
- [13] T. Greiner, H. Mark, G. T. Michael, W. M. Wing, Q. Z. Bin, *Nature Materials*, **1**, 76 (2012).
- [14] X. Xi., Q. L. Meng, F. X. Li, Y. Q. Ding, J. J. Ji, Z. R. Shi, G. H. Li, *Solar Energy Materials and Solar Cells*, **94**, 924 (2010).
- [15] J. S. Yu, N. N. Wang, Y. Zang, Y. D. Jiang, *Solar Energy Materials and Solar Cells*, **95**, 664 (2011).
- [16] Y. L. Wang, L. Y. Yang, C. Yao, W. J. Qin, S. G. Yin, F. L. Zhang, *Solar Energy Materials and Solar Cells*, **95**, 1243 (2011).
- [17] M. W. Shin, H. C. Lee, J. G. Lee, Y. Kim, Y. Y. Jung, S. Kim, *Thin Solid Films*, **363**, 302 (2000).
- [18] K. Aran, L. Hyemi, R. Choonghan, C. S. Min, C. Heeyeop, *Journal of Nanoscience*, **10**, 3326 (2010).
- [19] E. H. Kim, C. W. Yang, J. W. Park, *Current Applied Physics*, **10**, S510 (2010).
- [20] Y. C. Huang, Y. C. Liao, S. S. Li, M. C. Wu, C. W. Chen, W. F. Su, *Solar Energy Materials and Solar Cells*, **93**, 888 (2009).
- [21] A. Twardowski, *Physics Letters*, **94A**, 103 (1983).
- [22] A. M. Saleh, A. K. Hassan, R. D. Gould, *Journal of Physics and Chemistry of Solids*, **64**, 1297 (2003).
- [23] J. G. Simmons, *Conduction in thin dielectric films*, *J. Phys. D: Applied Physics*, **4**, 6130 (1971).
- [24] W. L. Ma, C. Y. Yang, X. Gong, K. Lee, A. J. Heeger, *Advanced Functional Materials* **15**, 1617 (2005).
- [25] F. C. Krebs, H. Spanggaard, *Chemical Material*, **17**, 5235 (2005).
- [26] F. C. Krebs, S. A. Gevorgyan, B. Gholamkhash, et al., *Solar Energy Material and Solar Cells*, **93**, 1968 (2009).
- [27] F. C. Krebs, J. E. Carle, N. Cruys-Bagger, M. Andersen, M. R. Lilliedal, M. A. Hammond, S. Hvidt, *Solar Energy Material and Solar Cells*, **86**, 499 (2005).
- [28] F. C. Krebs, *Solar Energy Material and Solar Cells*, **92**, 715 (2008).
- [29] K. Kawano, R. Pacios, D. Poplavskyy, J. Nelson, D. D. C. Bradley, J. R. Durrant, *Solar Energy Material and Solar Cells*, **90**, 3520 (2006).
- [30] A. M. Saleh, R. D. Gould, A. K. Hassan, *Physics State Solid*, **139**, 379 (1993).
- [31] X. Xi, W. J. Li, J. Q. Wu, *Solar Energy Materials and Solar Cells*, **94**, 2435 (2010).
- [32] G. Dennler, M. C. Scharber, C. J. Brabec, *Advanced Materials*, **13**, 1323 (2009).
- [33] S. D. Oosterhout, M. M. Wienk, S. S. Bavel, R. Thielmann, L. J. A. Koster, J. Gilot, J. Loos, V. Schmidt, R. A. J. Janssen, *Nature Materials*, **8**, 818 (3009).
- [34] L. Thrane, M. J. Thomas, J. Mikkel, F. C. Krebs, *Solar Energy Materials and Solar Cells*, **97**, 181 (2012).

---

\*Corresponding author: guohua\_li55@yahoo.com